A sight for sore eyes : assessing oncogenic functions of Hdmx and reactivation of p53 as a potential cancer treatment

Lange, J. de

Chapter 5

Chk2 mediates RITA-induced apoptosis

J. de Lange, M. Verlaan-de Vries, A.F.A.S. Teunisse, A.G. Jochemsen

Department of Molecular Cell Biology, Leiden University Medical Center, 2300 RC Leiden, The Netherlands

Cell Death and Differentiation 2012, *in press*

Abstract

Reactivation of the p53 tumor suppressor protein by small-molecules like Nutlin-3 and RITA (reactivation of p53 and induction of tumor cell apoptosis) is a promising strategy for cancer therapy. The molecular mechanisms involved in the responses to RITA remain enigmatic. Several groups reported the induction of a p53-dependent DNA damage response. Furthermore, the existence of a p53-dependent S-phase checkpoint has been suggested, involving the checkpoint kinase Chk1. We have recently shown synergistic induction of apoptosis by RITA in combination with Nutlin-3, and we observed concomitant Chk2 phosphorylation. Therefore, we investigated whether Chk2 contributes to the cellular responses to RITA. Strikingly, the induction of apoptosis seemed entirely Chk2-dependent. Transcriptional activity of p53 in response to RITA required the presence of Chk2. A partial rescue of apoptosis observed in Noxa knockdown cells emphasized the relevance of p53 transcriptional activity for RITA-induced apoptosis. In addition, we observed an early p53- and Chk2-dependent block of DNA replication upon RITA treatment. Replicating cells seemed more prone to entering RITA-induced apoptosis. Furthermore, the RITA-induced DNA damage response, which was not a secondary effect of apoptosis induction, was strongly attenuated in cells lacking p53 or Chk2. In conclusion, we identified Chk2 as an essential mediator of the cellular responses to RITA.

Introduction

The human transcription factor p53 provides an essential roadblock against cancer. The *TP53* gene is mutated in ~ 50% of all human cancers; the remaining tumors are assumed to have attenuated wild-type p53 activity (1). Reactivation of p53 in tumors with intact, but functionally impaired, p53 using non-genotoxic drugs is a promising anti-cancer strategy. Such strategies generally rely on inhibiting the interaction of p53 with its main negative regulators, human double minute 2 (Hdm2) and human double minute x (Hdmx). In addition, RITA (reactivation of p53 and induction of tumor cell apoptosis) was identified to directly bind and activate human p53 and to suppress *in vivo* growth of transformed cells in a p53-dependent manner (2).

Understanding factors that determine the outcome of p53 activation is the aim of many investigators, as specifically directing the cellular response towards apoptosis is crucial for successful cancer treatment. Interestingly, distinct p53-activating drugs have strongly divergent effects. For example, Nutlin-3 (3) and MI-219 (4) mainly induce G1 and G2-arrest, resulting in depletion of S-phase cells, whereas the induction of apoptosis by these compounds varies greatly between cell lines. On the other hand, RITA does not induce G1-arrest, but in general is more capable of inducing apoptosis (5). The mechanistic properties of RITA seem complex. RITA was proposed to induce a conformational change in p53 that prevents its binding to Hdm2 (2). NMR studies did not support this mechanism (6), but a later study suggested a role for the released pool of Hdm2 to promote degradation of p21 and the p53 cofactor hnRNP K (5). Furthermore, induction of pro-apoptotic homeodomain-interacting protein kinase-2 levels (7), inhibition of pro-survival TrxR1 activity (8) and reduced expression of Wip1 phosphatase and Hdmx (9) have been described as contributing to the RITA effects. RITA has also been implicated in inhibition of angiogenesis-promoting HIF-1α protein synthesis by increasing the phosphorylation of eIF2α (10). Importantly, several groups recently reported the induction of a DNA damage response by RITA (9-12)

The canonical DNA damage response network is traditionally divided into two major pathways, involving the sensor kinases ataxia telangiectasia mutated (ATM) and ataxia telangiectasia and Rad3-related (ATR) that activate their respective effector kinases, Chk2 and Chk1. ATR phosphorylates Chk1 on Ser317 and Ser345 (13, 14). The best characterized activating phosphorylation site of Chk2 is Thr68 (15), but phosphorylation of residues Ser19, Ser33 and Ser35 has been described to contribute to Chk2 activation (16). The p53 pathway is strongly affected at multiple levels by DNA damage signaling. ATM, ATR, Chk1

and Chk2 were all reported to directly mediate N-terminal phosphorylation on p53. In addition, both Hdm2 and Hdmx are downstream targets of the DNA damage response, including phosphorylation by ATM, ATR, Chk2 and Chk1 (Meek DW (17) and references therein).

The intensive interactions described above predict a great impact of DNA damage signaling on the biochemical and biological effects of small-molecule p53 activators. Indeed, when combined with genotoxic drugs like doxorubicin or topotecan, Nutlin-3 synergistically induced apoptosis in certain experimental settings (12, 18-20). We along with others showed synergistic tumor cell killing when Nutlin-3 and RITA are combined (12, 21), suggesting the induction of distinct pathways, as enhanced activation of the same pathway would expected to be additive at the best. Recently, RITA was proposed to induce p53-dependent replication stalling, with a role for Chk1 in maintaining DNA integrity, but not in the induction of apoptosis (11). In this study, we focused on the role of Chk2 in the RITA response and found that Chk2 is essential for the induction of replication arrest and apoptosis by RITA.

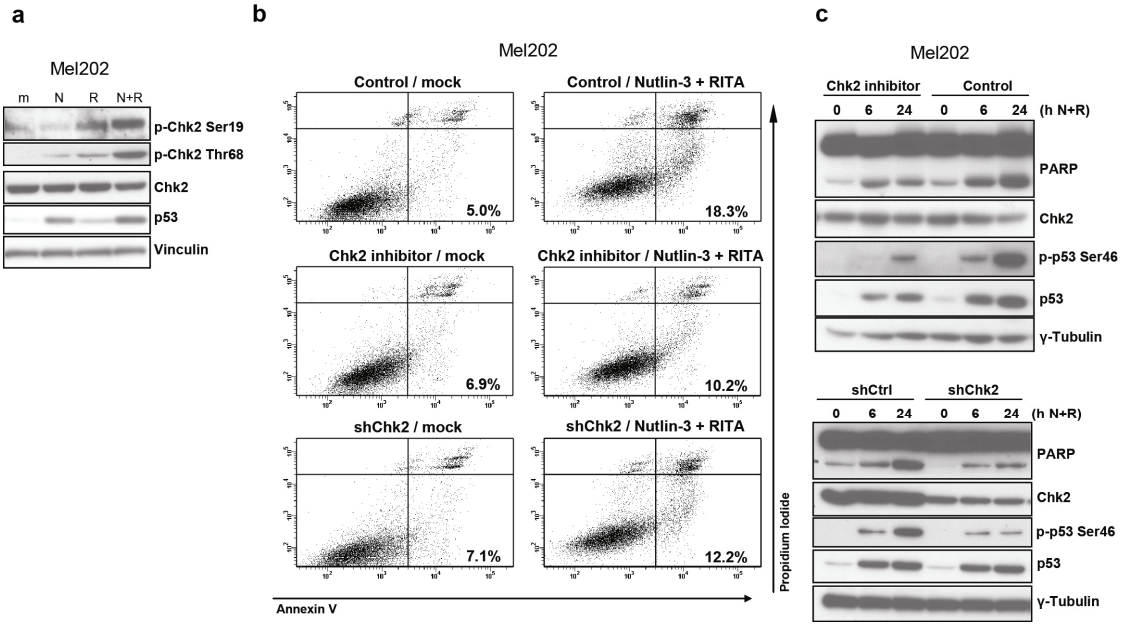

Figure 1 Chk2 inhibition attenuates apoptosis induction by RITA in Mel202 cells. (**a**) Mel202 cells were treated as indicated for 24 h and protein extracts were analyzed by western blotting using the indicated antibodies. (**b**) Mel202 cells were stably transduced with shCtrl or shChk2 constructs. Control cells were pre-treated for 2 h with the 10 μM Chk2 inhibitor II where indicated. Subsequently, cells were mock-treated or treated with a combination of Nutlin-3 and RITA. Apoptosis was assessed after 48 h by Annexin V staining. (**c**) Protein extracts from the same cells as in panel **b** were isolated after 24 h and analyzed by western blot using the indicated antibodies

Results

We recently reported that Nutlin-3 and RITA synergistically induce apoptosis in uveal melanoma cells, correlating with induction of ATM signaling and enhanced p53-Ser46 phosphorylation (12). An important downstream target of ATM is the checkpoint kinase Chk2. Indeed, Chk2 was phosphorylated on Thr68 and Ser19 upon RITA treatment in the uveal melanoma cell line Mel202 (Figure 1a). Therefore, we investigated whether Chk2 contributes to the RITA response, using a specific inhibitor of Chk2 kinase activity, and by short-hairpin RNA (shRNA)-mediated Chk2 knockdown. Interestingly, both approaches markedly reduced apoptosis induction by Nutlin-3 plus RITA in Mel202 cells, shown by Annexin V staining (Figure 1b) and poly [ADP-ribose] polymerase (PARP) cleavage (Figure 1c). Reduced apoptosis correlated with reduced p53-Ser46 phosphorylation. Similar results were obtained in 92.1, another uveal melanoma cell line (data not shown).

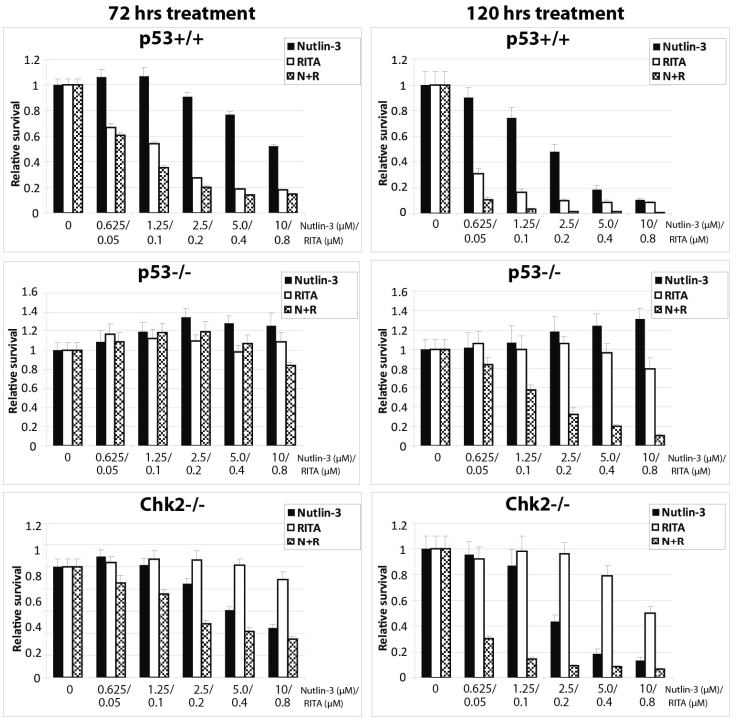

Drug concentrations		Combination Index	
Nutlin-3 (μM)	RITA (μM)	72h	120h
0.625	0.05	0.885	0.234
1.25	0.1	0.569	0.109
2.5	0.2	0.496	0.093
50	0.4	0.644	0.160
10	0.8	1.308	0.224

Figure 2 HCT116 $p53^{-/-}$ and HCT116 $Chk2^{-/-}$ cells show reduced sensitivity to RITA-induced growth inhibition. HCT116 $p53^{+/+}$, $p53^{-/-}$ and $Chk2^{-/-}$ cells were continuously treated for 72 h or 120 h as indicated with different concentrations of Nutlin-3 and RITA, alone or in constant ratio combinations. Cell viability was measured using the WST-1 proliferation assay. The effects of drug treatment as fraction of mock-treated control cells were calculated. The combination index (CI), reflecting the extent of synergy or antagonism for two drugs, was derived for HCT116 $p53^{+/+}$ cells after 72 h and 120 h treatments for each concentration of drug combination using Compusyn software (38). CI<0.9, synergy; 0.9<CI<1.1, additive effect; CI>1.1, antagonism

To further study the role of Chk2 in the responses to Nutlin-3 and RITA, we used the isogenic $p53^{+/+}$, $p53^{-/-}$ and $Chk2^{-/-}$ HCT116 colon carcinoma cell lines. We confirmed synergy between Nutlin-3 and RITA in wild-type HCT116 cells (Figure 2). Calculated combination index (CI) values indicated synergy at most concentrations. Notably, CI calculations as defined by Chou (22) require experimentally derived values describing the dose-response curves for each single drug, which is not possible if the drug has no detectable effect at all. As expected, $p53^{-/-}$ cells were largely insensitive to both treatments. Interestingly, whereas the sensitivity of $Chk2^{-/-}$ cells to Nutlin-3 was comparable to $p53^{+/+}$ cells, they were hardly affected by RITA. Only after 5 days of continuous RITA treatment, we could observe a clear effect in $Chk2^{-/-}$ cells at the highest concentrations. Remarkably, at this time point also the $p53^{-/-}$ cells were growth inhibited by the combination treatment, indicating activation of p53-independent pathways.

To obtain more insight into the effects of RITA and Nutlin-3 alone and in combination, we investigated the effects on cell cycle profiles (Figure 3a). In wild-type HCT116 cells, Nutlin-3 treatment induced both a G1 and a G2 arrest, whereas RITA treatment resulted in decreased G1 and increased S and G2/M fractions. RITA also prevented the S-phase depletion by Nutlin-3, suggesting an S-phase arrest by RITA. In $p53^{-/-}$ cells, Nutlin-3 alone had no effect, but RITA clearly decreased G1 and increased G2/M fractions. Combining Nutlin-3 and RITA dramatically elevated the G2/M fraction, which can explain the growth inhibition observed in the WST-1 assay (Figure 2). These findings indicate that Nutlin-3 and RITA exert some p53-independent effects, although the effect of Nutlin-3 is only revealed in the presence of RITA. In $Chk2^{-/-}$ cells, Nutlin-3 depleted the S phase and increased G1, but not G2/M, suggesting that Nutlin-3 induced G2-arrest is Chk2 dependent. In contrast to Nutlin-3, RITA decreased G1 and increased G2/M fractions, similar as observed in $p53^{-/-}$ cells. The combined treatment depleted S phase and arrested $Chk2^{-/-}$ cells in both G1 and G2. Notably, RITA alone hardly changed the percentage of cells in the S phase in $p53^{-/-}$ and $Chk2^{-/-}$ cells, whereas the G2/M increase was transient (data not shown). In conclusion, the cell-cycle profiles suggest that Nutlin-3 induces a p53-dependent G1 arrest and a p53- and Chk2-dependent G2 arrest. However, RITA induces a p53- and Chk2-dependent S arrest and a p53- and Chk2-independent G2 arrest, but no G1 arrest.

We also examined apoptosis induction using sub-G1 evaluation (Figure 3b) and Annexin V staining (Figure 3c). Nutlin-3 induced a mild, p53-dependent apoptotic response in HCT116. Importantly, RITA strongly induced apoptosis in a p53- and Chk2-dependent manner. Combination treatments, as compared with single RITA treatments, slightly increased apoptosis in all cell lines.

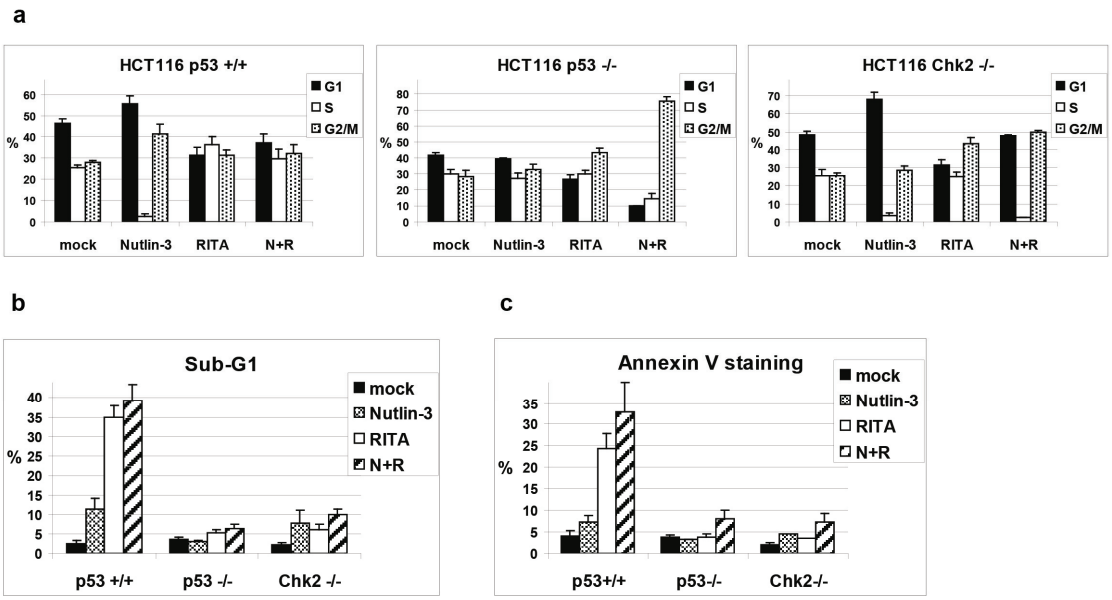

Figure 3 p53- and Chk2-dependent and -independent effects of Nutlin-3 and RITA on cell cycle profiles and apoptosis. (**a** and **b**) HCT116 $p53^{+/+}$, $p53^{-/-}$ and $Chk2^{-/-}$ cells were treated as indicated for 24 h, harvested and analyzed by flow cytometry. Bars represent means and s.e. of three independent experiments. (**c**) Cells were treated as indicated for 48 h, harvested and analyzed by Annexin V staining. Bars represent means and s.e. of three independent experiments

To obtain more insight into the pathways by which RITA affects cell-cycle progression and apoptosis, we analyzed the levels and phosphorylation status of a number of proteins (Figure 4a). Supporting the observed effects on apoptosis, RITA induced PARP cleavage in $p53^{+/+}$ cells, but not in $p53^{-/-}$ and $Chk2^{-/-}$ cells. As reported before (9-12), RITA also induced a DNA damage response, evidenced by phosphorylation of ATM-Ser1981, KRAB-interacting protein 1 (KAP1)-Ser824, Chk2-Thr68, p53-Ser15 and p53-Ser46, as well as by downregulation of Hdmx. Interestingly, these effects were strongly attenuated in $p53^{-/-}$ and $Chk2^{-/-}$ cells. In addition, Chk1-Ser345 phosphorylation, recently implicated in RITA response (11), and Hdm2 downregulation were all p53 and Chk2 dependent (Figure 4b). It is important to note that not only stress-induced p53 phosphorylation is strongly reduced in $Chk2^{-/-}$ cells, but also p53 stabilization (Figure 4b). We further analyzed the DNA damage response in HCT116 $p53^{+/+}$ cells in a RITA time course, in comparison with the known DNA-damaging agent etoposide (Figure 4c). RITA-induced phosphorylations clearly occurred with slower kinetics. Notably, phosphorylation of ATM, KAP1 and Chk2 induced by etoposide was comparable in $p53^{+/+}$, $p53^{-/-}$ and $Chk2^{-/-}$ cells (Supplementary Figure 1 and not shown), suggesting that the mechanisms by which RITA and etoposide elicit DNA damage response are distinct.

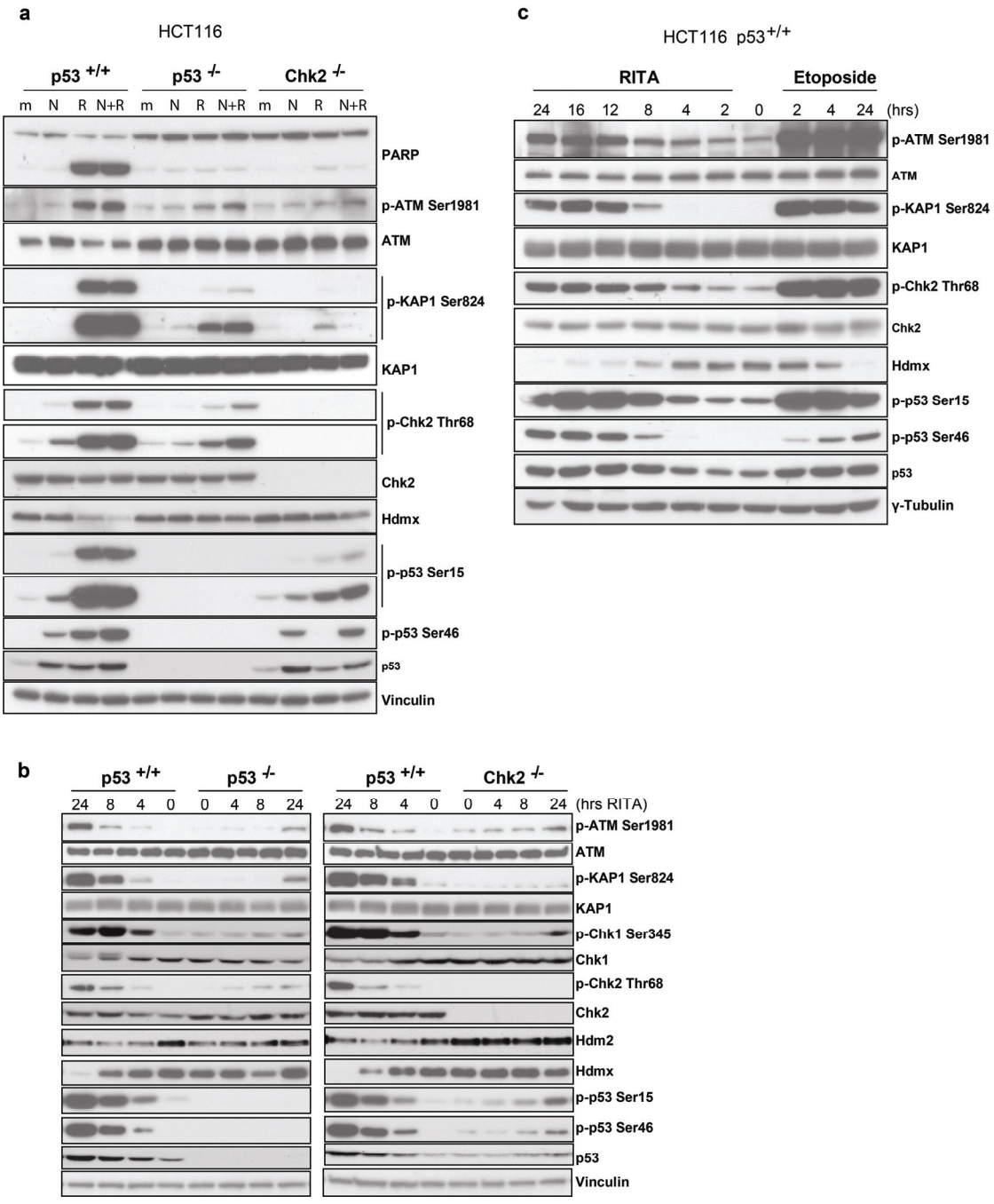

Figure 4 Activation of DNA damage response by RITA is p53- and Chk2-dependent and occurs with slower kinetics compared to etoposide. (**a**) HCT116 $p53^{+/+}$, $p53^{-/-}$ and $Chk2^{-/-}$ cells were treated as indicated for 24 h, and protein extracts were analyzed by western blot using the indicated antibodies. (**b**) HCT116 $p53^{+/+}$, $p53^{-/-}$ and $Chk2^{-/-}$ cells were treated as indicated, and protein extracts were analyzed by western blot using the indicated antibodies. (**c**) HCT116 $p53^{+/+}$ cells were treated with 1 μM RITA or 10 μM etoposide for the indicated periods, and protein extracts were analyzed by western blot using the indicated antibodies.

As the observed DNA damage response might be a secondary result of apoptosis-associated DNA fragmentation, we treated HCT116 cells with RITA in the presence of the pan-caspase inhibitor Z-VAD-FMK. Annexin V staining (Supplementary Figure 2a) and PARP cleavage (Supplementary Figure 2b) showed that Z-VAD-FMK efficiently blocked apoptosis induction by RITA and Nutlin-3 plus RITA. However, the inductions of ATM, KAP1, Chk2 and p53 phosphorylation, as well as Hdmx downregulation, were not influenced by Z-VAD-FMK. Furthermore, the RITA time course showed that PARP cleavage only became apparent after induction of the DNA damage response (compare Supplementary Figure 2c and Figure 4c).

Recently, it has been demonstrated that RITA blocks DNA replication in a p53-dependent manner (11). To test whether this effect depends on Chk2 expression, we analyzed 5-ethynyl-2'-deoxyuridine (EdU) incorporation in HCT116 $p53^{+/+}$, $p53^{-/-}$ and $Chk2^{-/-}$ cells in a RITA time course (Figure 5a). In $p53^{+/+}$ cells, 4-h RITA treatment already effectively blocked

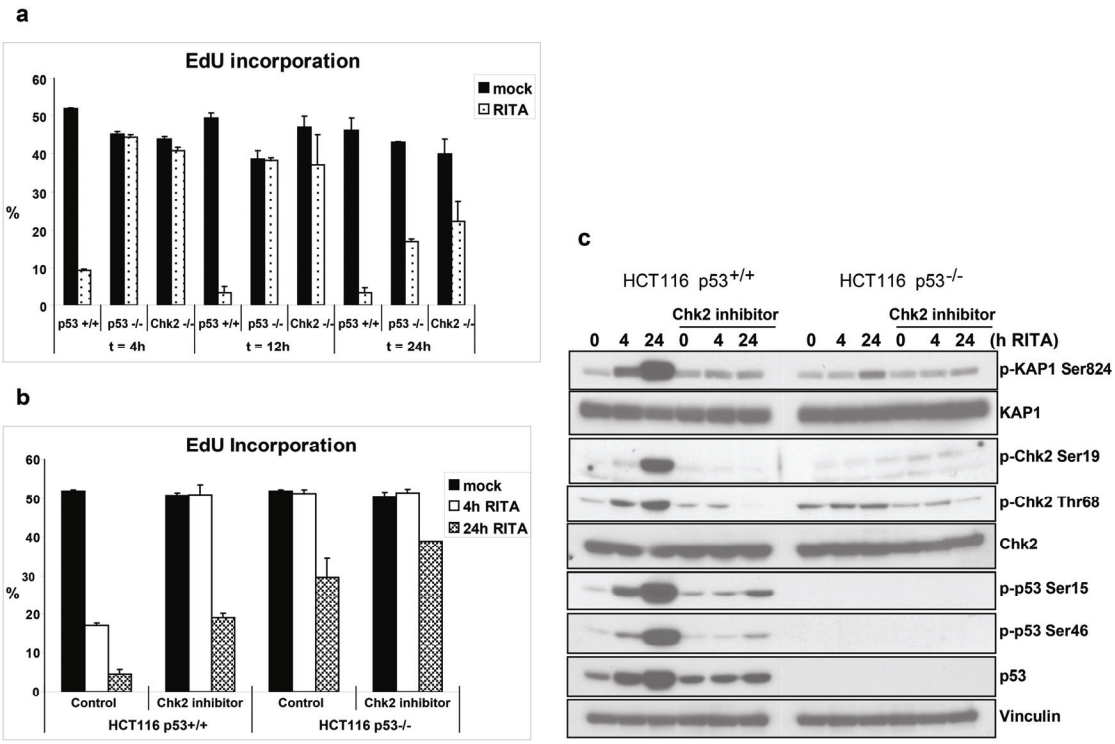

Figure 5 The rapid replication block in response to RITA treatment is p53- and Chk2 dependent. (**a**) HCT116 $p53^{+/+}$, $p53^{-/-}$ and $Chk2^{-/-}$ cells were treated with RITA for the indicated periods. Subsequently, 2.0 μM 5-ethynyl-2'-deoxyuridine (EdU) was added for 1 h to allow incorporation into newly synthesized DNA. Cells were harvested and percentages EdU positive cells were determined using flow cytometry. Bars represent means and s.e. of two independent experiments. (**b**) HCT116 $p53^{+/+}$ and $p53^{-/-}$ cells were pre-treated for 2 h with 10 μM Chk2 inhibitor II where indicated, and subsequently mock-treated or treated with RITA for 4 or 24 h. EdU incorporation was analyzed as described in panel **a**. (**c**) Protein extracts of cells treated as mentioned in panel **b** were analyzed by western blot using the indicated antibodies.

replication. The effects in $p53^{-/-}$ and $Chk2^{-/-}$ cells were much weaker; only after 24-h RITA treatment, a significant reduction in EdU-positive cells could be observed. A closer examination of the EdU profile at the 12-h time point (Supplementary Figure 3a) revealed that in $p53^{-/-}$ and $Chk2^{-/-}$ cells, RITA shifted the EdU-positive peak somewhat to the left, suggesting a slower DNA replication in these cells. To investigate whether Chk2 inhibition would modulate the effect of RITA on S-phase progression even in $p53^{-/-}$ cells, we chemically inhibited Chk2 kinase activity in HCT116 $p53^{+/+}$ and $p53^{-/-}$ cells and analyzed EdU incorporation (Figure 5b and Supplementary Figure 3b). In $p53^{+/+}$ cells, Chk2 inhibition prevented the replication block at 4 h, resembling the observations in $Chk2^{-/-}$ cells. In addition, the Chk2 inhibitor prevented phosphorylation of KAP1, Chk2 and p53, as well as p53 accumulation (Figure 5c). In $p53^{-/-}$ cells, Chk2 inhibition still partially rescued the effects of RITA on replication at later time points.

We hypothesized that RITA-induced apoptosis could be a secondary event of the replication block. If so, this could implicate that non-replicating cells are less prone to enter RITA-induced apoptosis. Therefore, we reduced the number of replicating cells by serum starvation (Figure 6a). Indeed, replicating cells seemed more sensitive to RITA treatment, as indicated by reduced Annexin V staining (Figure 6b, P=0.00284) and sub-G1 fraction (Figure 6c) in serum-deprived cells. Interestingly, reduced apoptosis did not coincide with lower induction of DNA damage response by RITA, with the exception of p53-Ser46 phosphorylation (Figure 6d). Notably, we found no protection from RITA by pre-treatment with Nutlin-3 in HCT116 cells (Supplementary Figure 4). In fact, in our hands, apoptosis induction by RITA was significantly enhanced by pre-treatment with Nutlin-3. This suggests that synergy between Nutlin-3 and RITA in apoptosis induction does not depend on DNA replication.

RITA promotes p53 transcriptional activity, including towards pro-apoptotic targets (5, 21). We analyzed the levels of several p53 target genes in response to RITA in different HCT116 cells (Figure 7a). RITA induced messenger RNA (mRNA) levels of p21 and Noxa and reduced MCL1 in HCT116 $p53^{+/+}$ cells. These alterations were not observed in $p53^{-/-}$ and $Chk2^{-/-}$ cells, indicating that the activation of p53-dependent transcription by RITA requires Chk2. Nutlin-3 induced transcription of p21, p53-upregulated modulator of apoptosis (PUMA) and Bax in $Chk2^{-/-}$ cells, indicating that these cells are still responsive to p53 activation (Supplementary Figure 5). It must be noted that we found only very low PUMA induction and no increase of Bax upon RITA treatment in HCT116 cells (Figure 7a), in line with our observation that HCT116 $PUMA^{-/-}$ and HCT116 $Bax^{-/-}$ cells were equally sensitive to RITA as were wild-type HCT116 cells (data not shown). To address the relevance of Noxa induction for RITA-induced apoptosis, we applied shRNA-mediated knockdown of Noxa expression. Noxa mRNA levels were efficiently

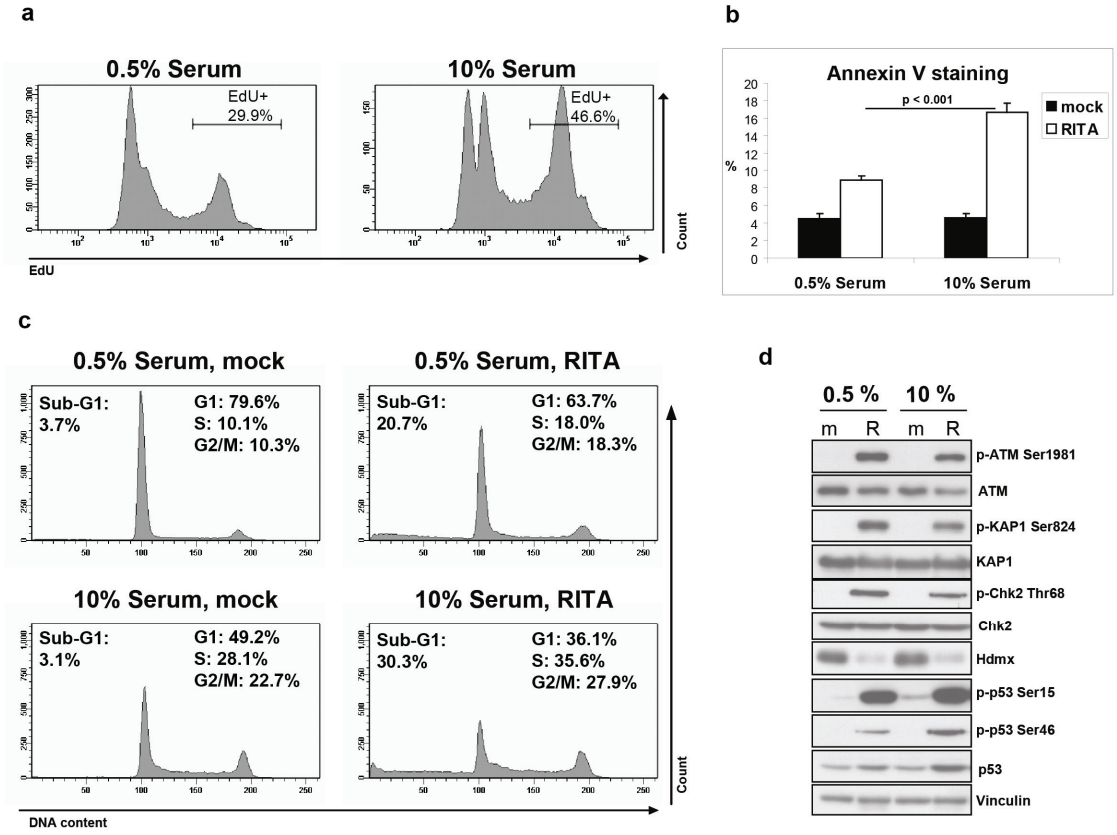

Figure 6 Serum-deprived cells show reduced RITA sensitivity. (**a**) HCT116 $p53^{+/+}$ cells were cultured in 0.5% serum for 48 h and DNA replication was analyzed using EdU incorporation. (**b-d**) Cells treated as mentioned in panel **a** were subsequently incubated with RITA for 24 h while maintaining initial serum conditions. (**b**) Apoptosis induction was assessed by Annexin V staining; bars represent means and s.e. of three independent experiments. Statistical analysis was performed using a two-tailed *t* test. (**c**) Cells were analyzed by flow cytometry. (**d**) Protein extracts were analyzed by western blot using the indicated antibodies.

reduced (Figure 7b), and RITA-induced apoptosis was significantly lower (P=0.0046, Figure 7c). These results suggest that the partial rescue of RITA-induced apoptosis by simultaneous knockdown of PUMA and Noxa (5) can be mainly attributed to the loss of Noxa-mediated effects.

We next investigated a causal link between RITA-induced DNA damage response and apoptosis by using two kinase inhibitors: KU-55933, which specifically inhibits ATM, and caffeine, which inhibits ATM, ATR and DNA-PK. Both diminished most of the RITA- and Nutlin-3 plus RITA-induced phosphorylation of ATM, KAP1, Chk2 and p53, as well as Hdmx downregulation (Supplementary Figure 6a). Interestingly, whereas KU-55933 efficiently blocked RITA-induced phosphorylation of ATM, Chk2 and KAP1, caffeine more efficiently inhibited p53-Ser46 phosphorylation. However, neither drug could rescue RITA-induced

cell death, as exemplified by PARP cleavage (Supplementary Figure 6a) and sub-G1 evaluation (Supplementary Figure 6b). In fact, both KU-55933 and caffeine enhanced induction of apoptosis. Treatment with either KU-55933 or caffeine did not affect RITA-induced mRNA levels of p21 and Noxa (data not shown).

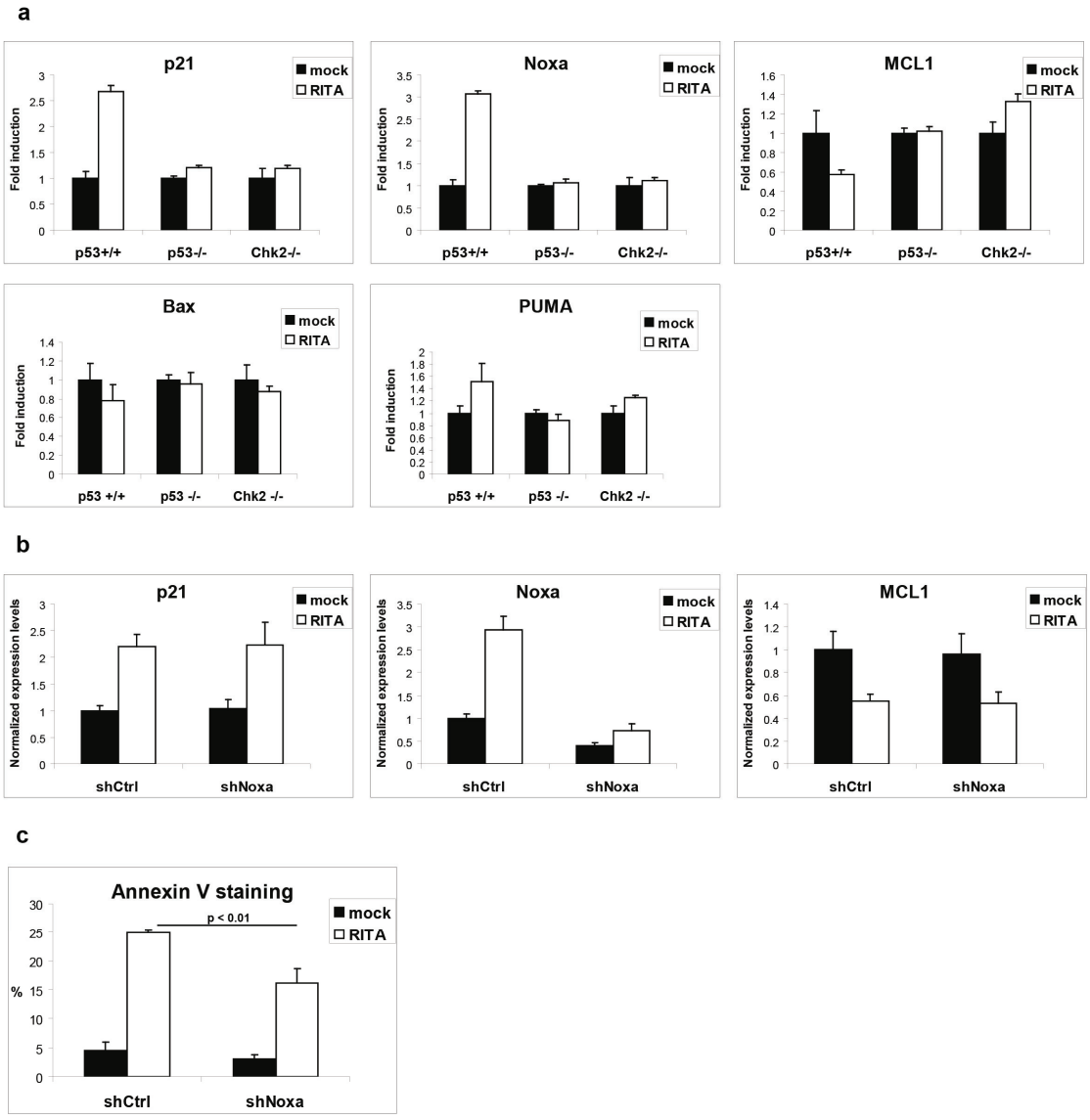

Figure 7 p53-dependent Noxa upregulation by RITA requires Chk2 and contributes to apoptosis induction. (**a**) HCT116 $p53^{+/+}$, $p53^{-/-}$ and $Chk2^{-/-}$ cells were treated with RITA for 6 h, and analyzed by qRT-PCR for p21, Noxa, MCL1, Bax and PUMA mRNA expression levels. (**b**) HCT116 cells stably expressing shCtrl or shNoxa constructs were treated with RITA for 6 h and analyzed by qRT-PCR. (**c**) HCT116 cells stably expressing shCtrl or shNoxa constructs were treated with RITA for 48 h and apoptosis was assessed using Annexin V staining. Bars represent means and s.e. of three independent experiments. Statistical analysis was performed using a two-tailed *t* test.

Recently, Wip1 downregulation was shown to contribute to RITA-induced apoptosis, at least partly through destabilization of Hdmx (9). We analyzed Wip1 mRNA expression in HCT116 cells (Figure 8a) and found that its reduction by RITA was both p53 and Chk2 dependent, correlating with Hdmx protein levels (Figure 4a). We further examined the role of Wip1 in RITA response using stable Wip1 knockdown in MCF7 cells and doxycycline-inducible Wip1 overexpression in U2OS cells. In MCF7 (Figure 8b), Wip1 knockdown indeed enhanced RITA--induced PARP cleavage, KAP1-Ser824 phosphorylation and Hdmx downregulation. *Vice versa*, Wip1 overexpression in U2OS indeed diminished RITA-induced PARP cleavage and phosphorylation of ATM, KAP1 and Chk2 (Figure 8c). Together, these results indicate that Chk2 contributes to the reduction of Wip1 levels after RITA treatment, and that Wip1 contributes to the modulation of the RITA response, as reported previously (9).

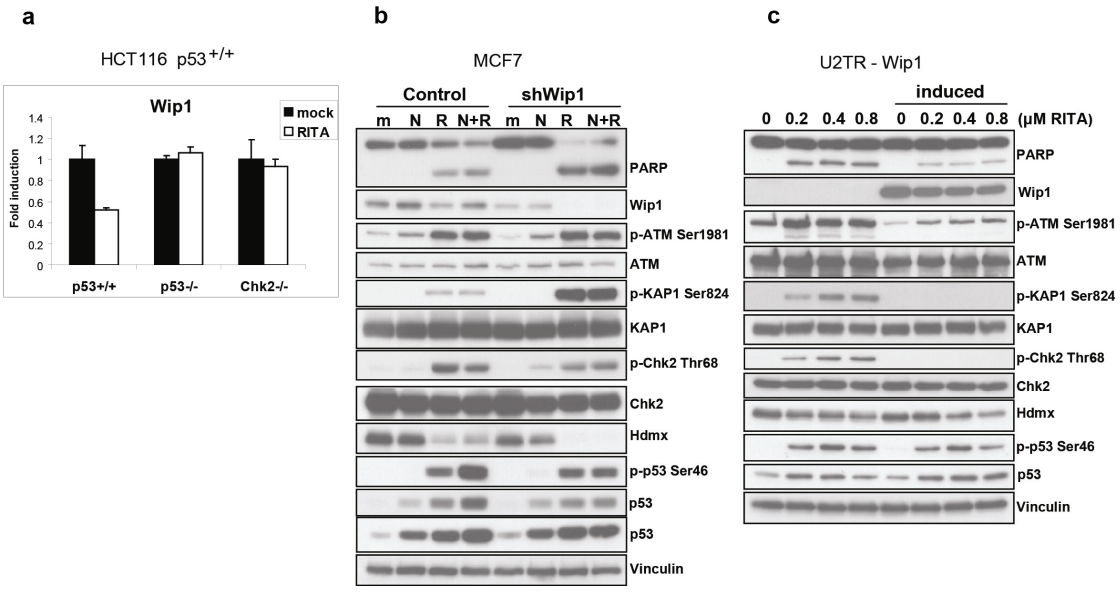

Figure 8 Chk2 contributes to the reduction of Wip1 levels after RITA treatment. (**a**) HCT116 $p53^{+/+}$, $p53^{-/-}$ and $Chk2^{-/-}$ cells were treated with RITA for 6 h, and RNA extracts were analyzed by qRT-PCR for Wip1 expression levels. (**b**) MCF7 cells stably transduced with an empty pRS vector or pRS-shWip1 were treated as indicated for 24 h, and protein extracts were analyzed by western blot using the indicated antibodies. (**c**) U2TR-Wip1 cells were pre-treated with 1 μg/ml doxycycline for 2 h to induce Wip1 expression, and subsequently treated for 6 h with the indicated doses RITA. Protein extracts were analyzed by western blot using the indicated antibodies.

Discussion

Several compounds have been developed for p53 reactivation in tumor cells to synergize with or even substitute conventional cancer therapies, including the small molecules Nutlin-3 (3) and RITA (2). They bind Hdm2 and p53, respectively, and interfere with the p53-Hdm2 interaction. However, the molecular changes that may be relevant for the cellular response, particularly those induced by RITA, stretch well beyond p53 stabilization. This is illustrated by the effects of RITA on the cell-cycle profile in HCT116 $p53^{-/-}$ cells, which was strongly enhanced by combination with Nutlin-3. However, the majority of RITA effects occur through p53, although the underlying mechanisms have not yet been completely elucidated.

Surprisingly, here we show that HCT116 $Chk2^{-/-}$ cells largely mimicked $p53^{-/-}$ cells in their RITA response: lack of immediate replication block, activation of DNA damage signaling, reduction of Hdm2 and Hdmx protein levels, transcriptional regulation of p53-responsive genes and, most importantly, induction of apoptosis. In contrast, $Chk2^{-/-}$ cells were still responsive to p53 activation by Nutlin-3 , although Nutlin-3 induced G2 arrest seemed Chk2 dependent. The absence of G2 arrest in $Chk2^{-/-}$ cells was restricted to Nutlin-3; RITA clearly (although transiently) elevated the G2/M fraction. This G2/M increase upon RITA treatment may appear stronger in $p53^{-/-}$ and $Chk2^{-/-}$ cells just because they lack an S-phase arrest. It has recently been demonstrated that RITA induces a p53-dependent S-phase checkpoint via stalling of replication fork elongation (11). The authors showed phosphorylation of Chk1 on Ser345 and proposed a functional contribution of Chk1, although this appeared to be restricted to maintaining DNA integrity upon short-term exposure, and the relevance of Ser345 phosphorylation remained unclear. Our data indicate that Chk2 is essential for both Chk1 phosphorylation and efficient activation of an S-phase checkpoint by RITA. It seems plausible that RITA-induced DNA damage signaling results from replication stalling. We found that RITA-induced phosphorylations occur with much slower kinetics as compared with a classical DNA damaging agent like etoposide. Furthermore, the DNA damage response is not just a result of apoptosis induction, as it was still observed in the presence of Z-VAD-FMK.

Which pathway does RITA use to trigger apoptosis? Although the mechanism by which RITA activates Chk2 has still to be solved, our data indicate that Chk2 is required for Hdm2 degradation and full p53 stabilization. This could implicate that RITA partly stabilizes p53 indirectly, by reducing Hdm2 levels. In addition, the partial rescue observed in Noxa knockdown experiments defined p53 transcriptional activity as an important contributor to

apoptosis induction upon RITA treatment. Furthermore, serum-starved cells displayed reduced sensitivity to RITA, suggesting that replicating cells are particularly prone to RITA-induced apoptosis. This may provide a valuable aspect of RITA as cancer treatment, as tumor cells generally replicate faster than normal cells. On the other hand, DNA replication seems not to be an absolute requirement for RITA-induced apoptosis. Pre-treatment of HCT116 cells with Nutlin-3 for 24 h, which effectively depleted S-phase cells, did not protect cells from RITA-induced apoptosis, in contrast to an earlier report in which U2OS cells were used (7). Replication blockage and apoptosis induction required the presence of both p53 and Chk2. These findings suggest that RITA activates a p53- and Chk2-dependent S-phase checkpoint that signals back to p53, possibly through Chk2, to activate a pro-apoptotic transcriptional program. However, DNA damage signaling may not be required for apoptosis induction, as serum starvation partially prevented apoptosis, but not the DNA damage response. Furthermore, the use of PIKK-inhibitors KU-55933 and caffeine revealed no evidence for a contribution of ATM/ATR/DNA-PK activity in RITA-induced apoptosis, supporting the findings of Ahmed *et al.* (11) obtained using Wortmannin. It must be noted that caffeine seemed much more efficient in inhibiting RITA-induced p53-Ser46 phosphorylation as compared with KU-55933, suggesting that this depends on ATR and/or DNA-PK activity, rather than on ATM. Interestingly, DNA-PK was reported to synergistically act with Chk2 to activate p53-dependent apoptosis (23).

We found that Chk2 kinase activity is required for activating both the early replication block and apoptosis after RITA treatment. Comparison of several time-course analyses suggests that phosphorylation of Chk2 is not necessary for inhibiting replication. Its contribution to apoptosis induction remains elusive. In addition, the relevant Chk2 substrate(s) need to be identified. An obvious candidate is p53-Ser46, which is believed to specifically lead to apoptosis (24, 25) and correlated with Nutlin-3 plus RITA-induced apoptosis in uveal melanoma (12). Indeed, RITA-induced p53-Ser46 phosphorylation was almost absent in HCT116 Chk2$^{-/-}$ cells. However, additional targets may be involved as well. Chk2 is known to phosphorylate proteins involved in cell cycle arrest, such as Cdc25C (26) and Cdc25A (27), and DNA repair, including BRCA1 (28). The most interesting Chk2 targets are those involved in apoptosis, which might include not only p53 and Hdmx but also E2F1 (29) and PML (30). However, we detected a reduction of E2F1 and its targets p73 and APAF1 on the mRNA level in response to RITA treatment in wild-type HCT116 cells, ruling out a putative involvement of E2F1.

Collective literature indicates that *Chk2* is a cancer-susceptibility gene, possibly acting in synergy with other factors to cause cancer (31). Patients with Chk2-deficient tumors might

be treated with inhibitors of other DNA-repair proteins, whereas patients with tumors harboring functional Chk2 may benefit from Chk2 inhibition. This relies on the observation that cancer cells often contain an impaired checkpoint machinery, which results in a greater dependence on the remaining functional processes that ensure cell survival. Indeed, Chk1 inhibitors aiming at potentiating DNA damaging chemotherapy have reached clinical trials (32). However, Chk2 inhibition is not always a good anti-cancer strategy. In fact, Chk2 activation in the absence of DNA damage was proposed as cancer therapy (33). In addition, Chk2 inhibition can protect cells from radiation toxicity; the Chk2 inhibitor VRX0466617 attenuated IR-induced apoptosis (34), and an earlier report showed that Chk2-deficient mice are radio resistant and exhibit impaired IR-induced p53-activation (35). This may be exploited to improve the therapeutic index of radiotherapy in Chk2-deficient tumors, as Chk2 could have a radio-protective effect on normal tissues.

Here, we show that Chk2 loss protects cells from RITA, indicating that RITA will be particularly useful in tumors harboring functional Chk2. Interestingly, we also found that Chk2 inhibition diminished apoptosis in uveal melanoma cell lines induced by a combination of Nutlin-3 and the topoisomerase I inhibitor Topotecan (data not shown). By contrast, inhibition of the ATR-Chk1 axis has been demonstrated to potentiate the effects of topoisomerase I inhibitors (36). Thus, Chk1 and Chk2 clearly exhibit distinct roles in the responses to replicative stress. Our data place Chk2 in a central position in mediating the cellular responses to RITA. Future work should focus on the mechanism by which RITA activates Chk2, as well as on precisely defining the S-phase checkpoint induced by RITA, which is confusing because its induction is p53 dependent. Another challenge is finding out through which substrate(s) Chk2 contributes to apoptosis induction. Convincing evidence that replication stalling really is the (only) trigger for apoptosis is still lacking, so in theory RITA might induce two separate events. Elucidating these issues will help understanding the mechanistic properties of RITA and the evaluation of its utility as anti-cancer drug.

Materials and Methods

Cell lines, lentiviral transductions

Human uveal melanoma cell line Mel202 was cultured in RPMI + F10 medium (1:1 ratio) with 10% fetal bovine serum (FBS) and antibiotics. Human colorectal carcinoma HCT116, human breast cancer cell line MCF7 and human osteosarcoma U2OS were cultured in Dulbecco's modified Eagle medium supplemented with 10% FBS and antibiotics. HCT116 $p53^{+/+}$, $p53^{-/-}$ and $Chk2^{-/-}$ cell lines were a kind gift from Dr. B. Vogelstein. The generation of U2OS cells with inducible Wip1 expression (U2TR) has

been described before (37). U2TR cells, as well as MCF7 cell lines stably transduced with empty pRS or pRS-shWip1 vectors, were kindly provided by Dr. R. Medema. Lentiviral constructs targeting Noxa (TRCN0000153637), Chk2 (TRCN0000010314) and a non-targeting control construct (SHC002) were obtained from the Mission shRNA library (Sigma-Aldrich, St Louis, MO, USA). Cells were transduced using MOI = 1.0 in a medium containing 8.0 μg/ml polybrene and puromycin selected for stable expression.

Drug treatments

HCT116 cells were seeded in 6-wells plates at a density of $5.0*10^5$ cells per well, Mel202 at $1.0*10^6$ cells per 6-cm dish, MCF7 at $9.0*10^5$ cells per 6-cm dish and U2TR at $6.0*10^5$ cells per 6-cm dish. Unless differently stated, final drug concentrations were 1.0 μM RITA and 10 μM Nutlin-3 in HCT116 and MCF7, and 0.25 μM RITA and 3.0 μM Nutlin-3 in Mel202. Nutlin-3 was purchased from Cayman Chemical (Ann Arbor, MI, USA) and RITA was kindly provided by Galina Selivanova. KU-55933 was a kind gift of Graeme Smith and Steve Jackson, and provided to us by Yosef Shiloh. Caffeine (C0750), Chk2 inhibitor II (C3742) and Z-VAD-FMK (V116) were purchased from Sigma-Aldrich.

Immunoblotting

Cells were lysed in Giordano buffer (50 mM Tris-HCl, pH 7.4, 250 mM NaCl, 0.1% Triton X-100, 5 mM EDTA) with protease- and phosphatase inhibitors. Proteins were separated by SDS-PAGE, blotted onto polyvinylidene fluoride transfer membranes, incubated with the appropriate primary (listed in Supplementary Table 1) and secondary antibodies, and bands were visualized by chemoluminescence (West Dura, Pierce Biotechnology, Rockford, IL, USA).

RNA isolation, quantitative real-time PCR

RNA was isolated using the SV Total RNA isolation kit (Promega, Madison, WI, USA). cDNA was synthesized using 2.0 μg RNA in a total volume of 30 μl reverse transcriptase reaction mixture (Promega). Samples were analyzed in triplicate using SYBR Green mix (Roche Biochemicals, Indianapolis, IN, USA) in a 7900ht Fast Real-Time PCR System (Applied Biosystems, Foster City, CA, USA). For normalization, the geometric mean of two housekeeping genes (*RPS11* and *CAPNS1*) was used. Expression levels were calculated relative to untreated samples. Primer sequences are listed in Supplementary Table 2.

Flow cytometry

Cells were harvested, washed in PBS and fixed in ice-cold 70% EtOH. Before to FACS analysis, cells were washed in PBS and resuspended in PBS containing 50 μg/ml RNase A and 50 μg/ml propidium iodide (PI). Flow cytometry was performed in the BD LSR II system (BD Biosciences, San Diego, CA, USA). For Annexin V staining, cells were washed twice in PBS and resuspended in Annexin V-binding buffer containing Fluorescein isothyocyanate (FITC)-labeled Annexin-V (Sigma-Aldrich) and PI. After 10-min RT incubation cells were analyzed by flow cytometry. Positive PI staining, indicating necrotic or late apoptotic cells were excluded from the analysis. PI-negative, Annexin V-positive cells represent early apoptotic cells.

For EdU incorporation, we used the Click-iT EdU flow cytometry assay kit (Invitrogen, Grand Island, NY, USA). In short, cells were 1h pulse-labeled with 2.0 μM EdU, harvested, fixed with 4% paraformaldehyde and permeabilized with a saponin-based reagent. Cells were stained with Alexa Fluor 488 azide and analyzed by flow cytometry to detect EdU positive cells.

WST-1 proliferation assay, calculation of synergism

HCT116 cells were counted and seeded in triplicate in 96-well plates at a density of 4000 cells per well, in a total volume of 100 μl medium. Cells were incubated with 10 μl WST-1 (Roche) for two hours and absorbance (450 nm) was measured in a microplate reader (Victor; Perkin Elmer, San Jose, CA, USA). For synergy studies, drug effects were calculated as 'affected fraction' of treated *versus* untreated cells. Dose-effect analyses and calculation of CI were performed using CompuSyn software (Paramus, NJ, USA (38)). CI reflects the extent of synergy or antagonism for two drugs: CI<0.9, synergy; 0.9<CI<1.1, additive effect; CI>1.1, antagonism.

Acknowledgements

We thank Prof. B.R. Ksander for providing the Mel202 cell line, Dr. B Vogelstein for providing the HCT116 cell lines, Dr. R. Medema for the MCF-7/pRS, MCF-7/pRS-shWip1 cells and the Wip1-inducible U2OS cells U2TR, as well as Dr. G. Selivanova for providing RITA.

Reference List

(1) Vogelstein B, Lane D, Levine AJ. Surfing the p53 network. *Nature* 2000; **408**: 307-310.

(2) Issaeva N, Bozko P, Enge M, Protopopova M, Verhoef LG, Masucci M, et al. Small molecule RITA binds to p53, blocks p53-HDM-2 interaction and activates p53 function in tumors. *Nat Med* 2004; **10**: 1321-1328.

(3) Vassilev LT, Vu BT, Graves B, Carvajal D, Podlaski F, Filipovic Z, et al. In vivo activation of the p53 pathway by small-molecule antagonists of MDM2. *Science* 2004; **303** :844-848.

(4) Ding K, Lu Y, Nikolovska-Coleska Z, Wang G, Qiu S, Shangary S, et al. Structure-based design of spiro-oxindoles as potent, specific small-molecule inhibitors of the MDM2-p53 interaction. *J Med Chem* 2006; **49**: 3432-3435.

(5) Enge M, Bao W, Hedstrom E, Jackson SP, Moumen A, Selivanova G. MDM2-dependent downregulation of p21 and hnRNP K provides a switch between apoptosis and growth arrest induced by pharmacologically activated p53. *Cancer Cell* 2009; **15**: 171-183.

(6) Krajewski M, Ozdowy P, D'Silva L, Rothweiler U, Holak TA. NMR indicates that the small molecule RITA does not block p53-MDM2 binding in vitro. *Nat Med* 2005;**11**: 1135-1136.

(7) Rinaldo C, Prodosmo A, Siepi F, Moncada A, Sacchi A, Selivanova G, et al. HIPK2 regulation by MDM2 determines tumor cell response to the p53-reactivating drugs nutlin-3 and RITA. *Cancer Res* 2009; **69**: 6241-6428.

(8) Hedstrom E, Eriksson S, Zawacka-Pankau J, Arner ES, Selivanova G. p53-dependent inhibition of TrxR1 contributes to the tumor-specific induction of apoptosis by RITA. *Cell Cycle* 2009 ;**8**: 3576-3583.

(9) Spinnler C, Hedstrom E, Li H, De Lange J, Nikulenkov F, Teunisse AF, et al. Abrogation of Wip1 expression by RITA-activated p53 potentiates apoptosis induction via activation of ATM and inhibition of HdmX. *Cell Death Differ* 2011; **18**:1736-1745.

(10) Yang J, Ahmed A, Poon E, Perusinghe N, de Haven BA, Box G, et al. Small-molecule activation of p53 blocks hypoxia-inducible factor 1alpha and vascular endothelial growth factor expression in vivo and leads to tumor cell apoptosis in normoxia and hypoxia. *Mol Cell Biol* 2009; **29**: 2243-2253.

(11) Ahmed A, Yang J, Maya-Mendoza A, Jackson DA, Ashcroft M. Pharmacological activation of a novel p53-dependent S-phase checkpoint involving CHK-1. *Cell Death Dis* 2011; May 19; 2 :e160.

(12) De Lange J, Ly LV, Lodder K, Verlaan-de Vries M, Teunisse AF, Jager MJ, et al. Synergistic growth inhibition based on small-molecule p53 activation as treatment for intraocular melanoma. *Oncogene* 2011; Jul 18.

(13) Liu Q, Guntuku S, Cui XS, Matsuoka S, Cortez D, Tamai K, et al. Chk1 is an essential kinase that is regulated by Atr and required for the G(2)/M DNA damage checkpoint. *Genes Dev* 2000; **14**: 1448-1459.

(14) Zhao H, Piwnica-Worms H. ATR-mediated checkpoint pathways regulate phosphorylation and activation of human Chk1. *Mol Cell Biol* 2001; **21**: 4129-4139.

(15) Ahn JY, Schwarz JK, Piwnica-Worms H, Canman CE. Threonine 68 phosphorylation by ataxia telangiectasia mutated is required for efficient activation of Chk2 in response to ionizing radiation. *Cancer Res* 2000; **60**: 5934-5936.

(16) Buscemi G, Carlessi L, Zannini L, Lisanti S, Fontanella E, Canevari S, et al. DNA damage-induced cell cycle regulation and function of novel Chk2 phosphoresidues. *Mol Cell Biol* 2006; **26**: 7832-7845.

(17) Meek DW. Tumour suppression by p53: a role for the DNA damage response? *Nat Rev Cancer* 2009; **9**: 714-723.

(18) Coll-Mulet L, Iglesias-Serret D, Santidrian AF, Cosialls AM, de FM, Castano E, et al. MDM2 antagonists activate p53 and synergize with genotoxic drugs in B-cell chronic lymphocytic leukemia cells. *Blood* 2006; **107**: 4109-4114.

(19) Lam S, Lodder K, Teunisse AF, Rabelink MJ, Schutte M, Jochemsen AG. Role of Mdm4 in drug sensitivity of breast cancer cells. *Oncogene* 2010; **29**: 2415-2426.

(20) Laurie NA, Donovan SL, Shih CS, Zhang J, Mills N, Fuller C, et al. Inactivation of the p53 pathway in retinoblastoma. *Nature* 2006; **444**: 61-66.

(21) Saha MN, Jiang H, Mukai A, Chang H. RITA inhibits multiple myeloma cell growth through induction of p53-mediated caspase-dependent apoptosis and synergistically enhances nutlin-induced cytotoxic responses. *Mol Cancer Ther* 2010; **9**: 3041-3051.

(22) Chou TC. Theoretical basis, experimental design, and computerized simulation of synergism and antagonism in drug combination studies. *Pharmacol Rev* 2006; **58**: 621-681.

(23) Jack MT, Woo RA, Motoyama N, Takai H, Lee PW. DNA-dependent protein kinase and checkpoint kinase 2 synergistically activate a latent population of p53 upon DNA damage. *J Biol Chem* 2004; **279**: 15269-15273.

(24) Bulavin DV, Saito S, Hollander MC, Sakaguchi K, Anderson CW, Appella E, et al. Phosphorylation of human p53 by p38 kinase coordinates N-terminal phosphorylation and apoptosis in response to UV radiation. *EMBO J* 1999; **18**: 6845-6854.

(25) Saito S, Goodarzi AA, Higashimoto Y, Noda Y, Lees-Miller SP, Appella E, et al. ATM mediates phosphorylation at multiple p53 sites, including Ser(46), in response to ionizing radiation. *J Biol Chem* 2002; **277**: 12491-12494.

(26) Blasina A, de W, IV, Laus MC, Luyten WH, Parker AE, McGowan CH. A human homologue of the checkpoint kinase Cds1 directly inhibits Cdc25 phosphatase. *Curr Biol* 1999; **9**: 1-10.

(27) Falck J, Mailand N, Syljuasen RG, Bartek J, Lukas J. The ATM-Chk2-Cdc25A checkpoint pathway guards against radioresistant DNA synthesis. *Nature* 2001; **410**: 842-847.

(28) Lee JS, Collins KM, Brown AL, Lee CH, Chung JH. hCds1-mediated phosphorylation of BRCA1 regulates the DNA damage response. *Nature* 2000; **404**: 201-204.

(29) Stevens C, Smith L, La Thangue NB. Chk2 activates E2F-1 in response to DNA damage. *Nat Cell Biol* 2003; **5**: 401-409.

(30) Yang S, Kuo C, Bisi JE, Kim MK. PML-dependent apoptosis after DNA damage is regulated by the checkpoint kinase hCds1/Chk2. *Nat Cell Biol* 2002; **4**: 865-870.

(31) Antoni L, Sodha N, Collins I, Garrett MD. CHK2 kinase: cancer susceptibility and cancer therapy - two sides of the same coin? *Nat Rev Cancer* 2007; 7: 925-936.

(32) Ma CX, Janetka JW, Piwnica-Worms H. Death by releasing the breaks: CHK1 inhibitors as cancer therapeutics. *Trends Mol Med* 2011; **17**: 88-96.

(33) Chen CR, Wang W, Rogoff HA, Li X, Mang W, Li CJ. Dual induction of apoptosis and senescence in cancer cells by Chk2 activation: checkpoint activation as a strategy against cancer. *Cancer Res* 2005; **65**: 6017-6021.

(34) Carlessi L, Buscemi G, Larson G, Hong Z, Wu JZ, Delia D. Biochemical and cellular characterization of VRX0466617, a novel and selective inhibitor for the checkpoint kinase Chk2. *Mol Cancer Ther* 2007; **6**: 935-944.

(35) Takai H, Naka K, Okada Y, Watanabe M, Harada N, Saito S, et al. Chk2-deficient mice exhibit radioresistance and defective p53-mediated transcription. *EMBO J* 2002; **21**: 5195-5205.

(36) Flatten K, Dai NT, Vroman BT, Loegering D, Erlichman C, Karnitz LM, et al. The role of checkpoint kinase 1 in sensitivity to topoisomerase I poisons. *J Biol Chem* 2005; **280**: 14349-14355.

(37) Macurek L, Lindqvist A, Voets O, Kool J, Vos HR, Medema RH. Wip1 phosphatase is associated with chromatin and dephosphorylates gammaH2AX to promote checkpoint inhibition. *Oncogene* 2010; **29**: 2281-2291.

(38) CompuSyn software for drug combinations and for general dose-effect analysis, and user's guide [computer program]. ComboSyn, Inc.Paramus, NJ; 2007.

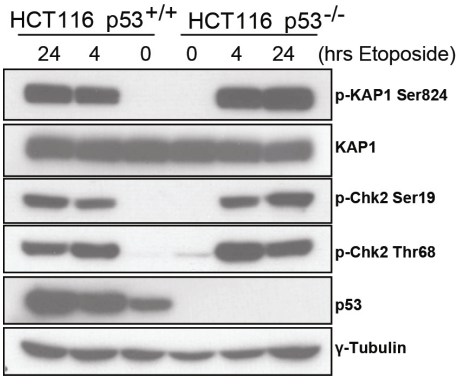

Supplementary Figure 1 Similar inductions of KAP1 and Chk2 phosphorylations in HCT116 $p53^{+/+}$ and $p53^{-/-}$ cells. HCT116 $p53^{+/+}$ and $p53^{-/-}$ cells were mock treated or treated with 10 μM etoposide for 4 or 24 h, and protein extracts were analyzed by western blot using the indicated antibodies.

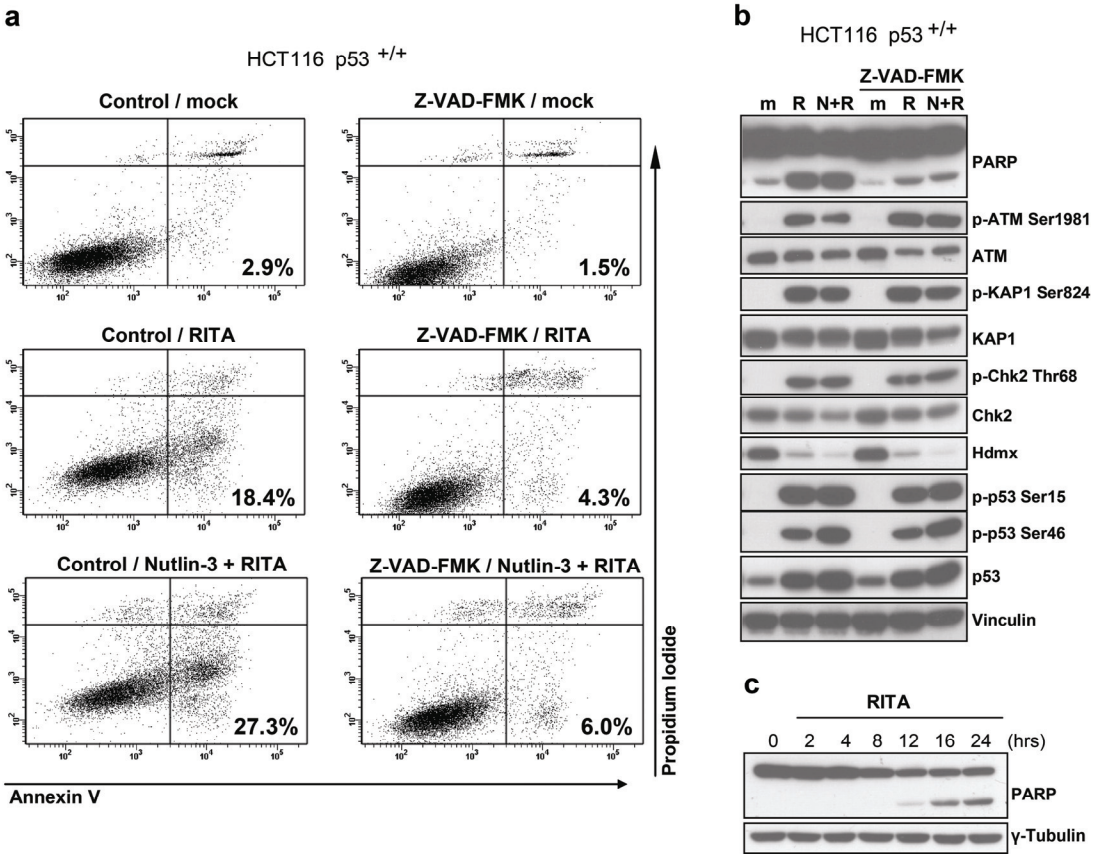

Supplementary Figure 2 Activation of DNA damage response by RITA is not a secondary effect caused by apoptosis induction. HCT116 $p53^{+/+}$, $p53^{-/-}$ and $Chk2^{-/-}$ cells were 2 h pre-treated with 20 μM Z-VAD-FMK and subsequently treated as indicated. (**a**) Apoptosis was assessed after 48 h using Annexin V staining. (**b**) Protein extracts were isolated after 24 h and analyzed by western blot using the indicated antibodies. (**c**) HCT116 $p53^{+/+}$ cells were treated with RITA for the indicated periods, and proteins were analyzed by western blot using the indicated antibodies.

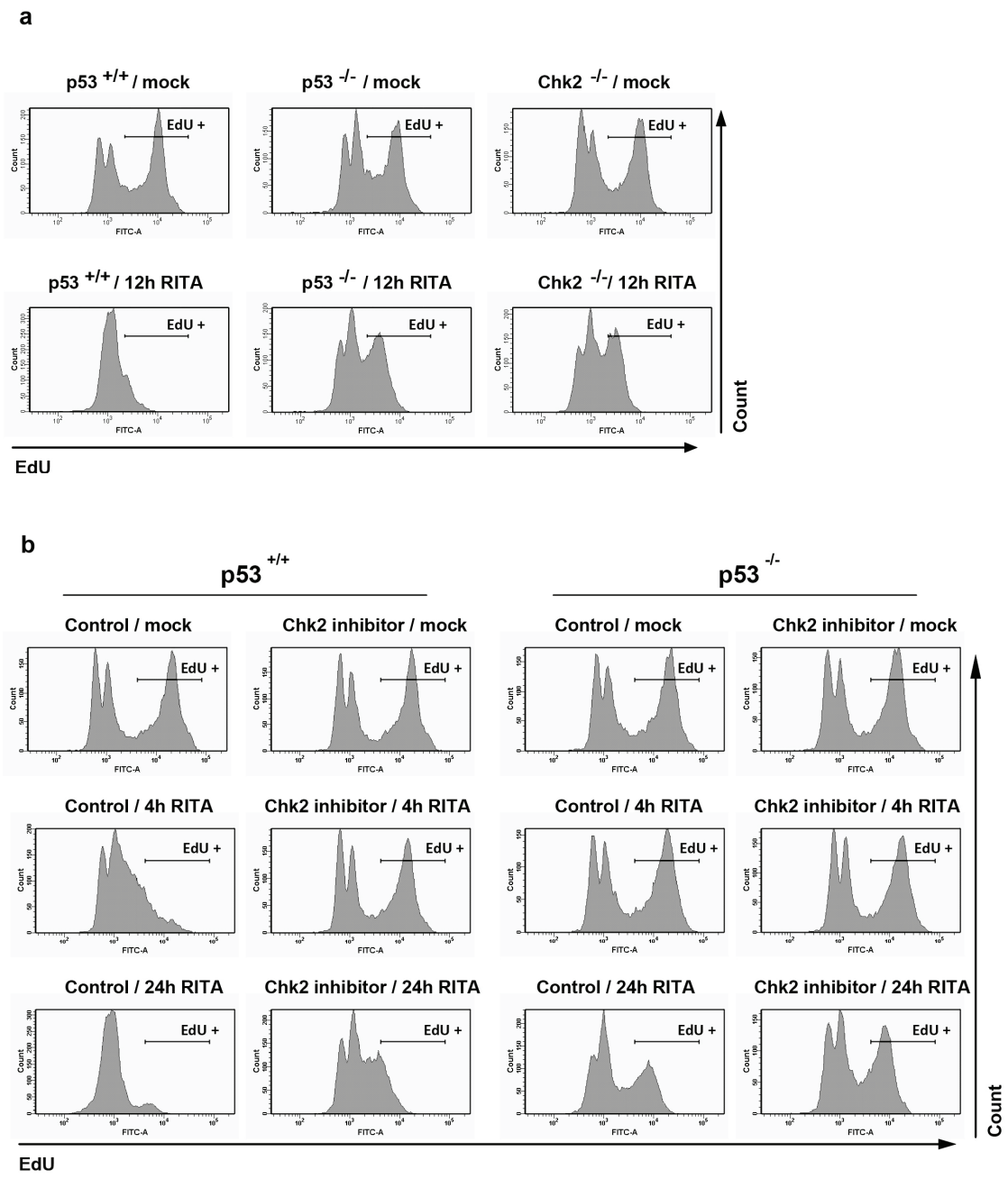

Supplementary Figure 3 RITA slows down DNA replication of p53- and Chk2-deficient HCT116 cells at later time points. (**a**) HCT116 $p53^{+/+}$, $p53^{-/-}$ and $Chk2^{-/-}$ cells were treated with RITA for 12 h. Subsequently, 5-ethynyl-2'-deoxyuridine (EdU) was added (final concentration 2.0 μM) for 1 h to allow incorporation into newly synthesized DNA. Cells were harvested and analyzed for EdU content using flow cytometry. (**b**) HCT116 $p53^{+/+}$ and $p53^{-/-}$ cells were pre-treated for 2 h with 10 μM Chk2 inhibitor II where indicated, and subsequently mock-treated or treated with RITA for 4 or 24 h. Cells were harvested and analyzed for EdU content using flow cytometry.

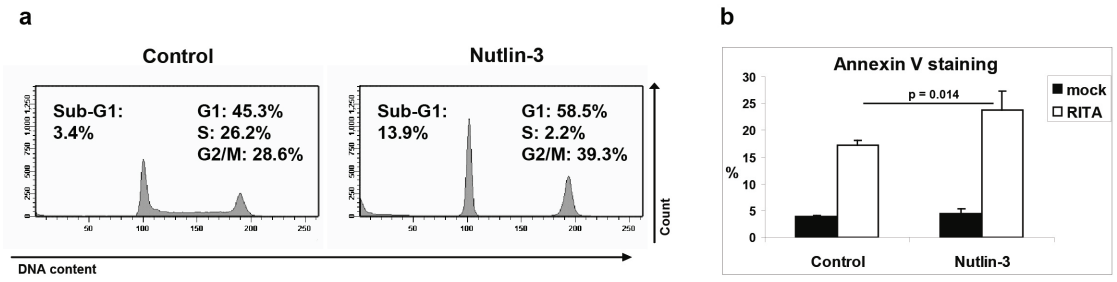

Supplementary Figure 4 Pre-treatment with Nutlin-3 does not protect HCT116 cells from apoptosis induction by RITA. (**a**) HCT116 $p53^{+/+}$ cells were 24 h pre-treated with 10 μM Nutlin-3 and the effect on cell-cycle distribution was analyzed using flow cytometry. (**b**) Cells were subsequently incubated with RITA for 24 h in the presence of Nutlin-3. Apoptosis induction was assessed by Annexin V staining; bars represent means and s.e. of four independent experiments. Statistical analysis was performed using a two-tailed *t* test.

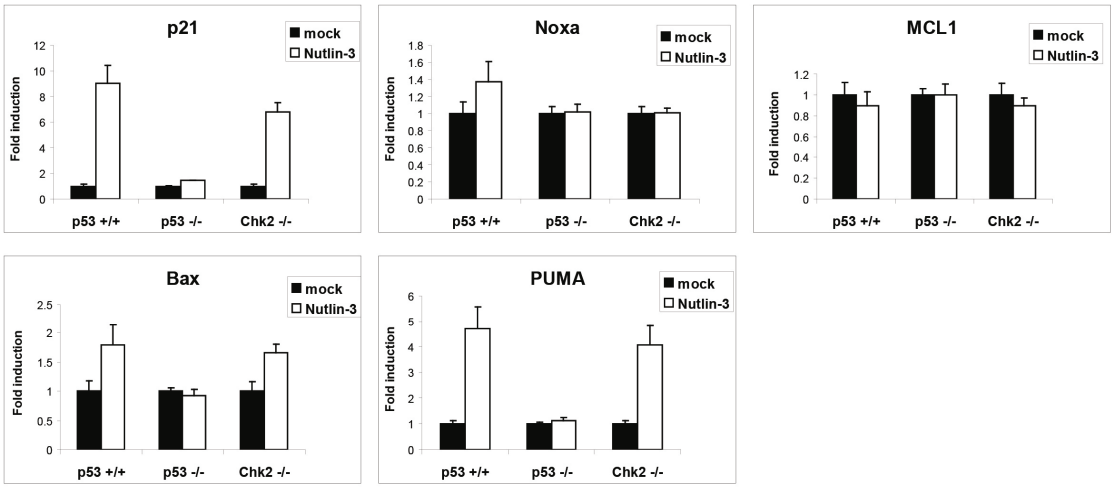

Supplementary Figure 5 Nutlin-3 induces transcription of p53 target genes in HCT116 $p53^{+/+}$ and $Chk2^{-/-}$ cells. HCT116 $p53^{+/+}$, $p53^{-/-}$ and $Chk2^{-/-}$ cells were treated with 10 μM Nutlin-3 for 6 h, and analyzed by qRT-PCR for p21, Noxa, MCL1, Bax and PUMA expression levels.

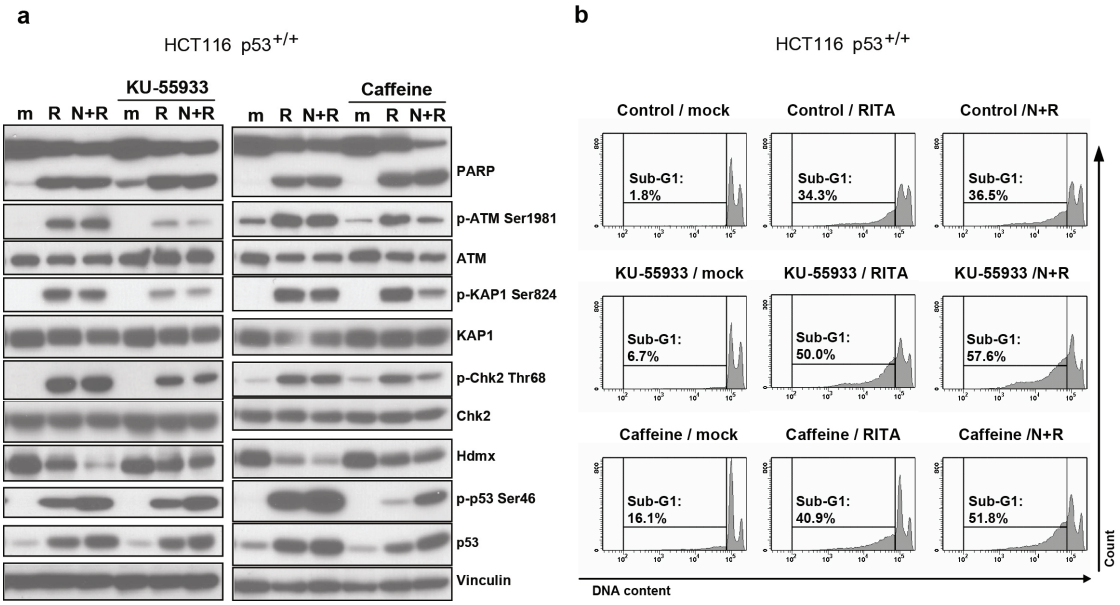

Supplementary Figure 6 Inhibition of RITA-induced DNA damage signaling fails to prevent apoptosis. HCT116 cells were 2 h pre-treated with 10 μM KU-55933 or 5 mM caffeine and subsequently treated for 24 h as indicated. (**a**) Protein extracts were analyzed by western blot using the indicated antibodies. (**b**) Cells were harvested and analyzed by flow cytometry for sub-G1 evaluation.

Supplementary Table 1: List of antibodies

Protein	Name/ cat. #	Company
PARP	9542	Cell signalling Technology, Beverly, MA, USA
p-ATM Ser1981	EP1890Y / 2152-1	Epitomics, California, USA
ATM	Y170 / 1549-1	Epitomics, California, USA
p-KAP1 Ser824	A300-767A	Bethyl Laboratories, Montgomery TX, USA
KAP1	A300-274A	Bethyl Laboratories, Montgomery TX, USA
p-Chk1 Ser345	2348	Cell signalling Technology, Beverly, MA, USA
Chk1	FL-476 / sc-7898	Santa Cruz Biotechnology, Santa Cruz, CA, USA
p-Chk2 Ser19	2666S	Cell signalling Technology, Beverly, MA, USA
p-Chk2 Thr68	C13C1 / 2197	Cell signalling Technology, Beverly, MA, USA
Chk2	EPR4325 / 3428-1	Epitomics, California, USA
Wip1	A300-664A	Bethyl Laboratories, Montgomery TX, USA
Hdm2 *	4B2	Chen *et al*., 1993
Hdm2 *	SMP14 sc-6965	Santa Cruz Biotechnology, Santa Cruz, CA, USA
Hdmx	A300-287A	Bethyl Laboratories, Montgomery TX, USA
p-p53 Ser46	2190-1 / EP42Y	Epitomics, California, USA
p-p53 Ser15	9284	Cell signalling Technology, Beverly, MA, USA
p53 °	DO-1 / sc-126	Santa Cruz Biotechnology, Santa Cruz, CA, USA
p53 °	PAb1801 / sc-98	Santa Cruz Biotechnology, Santa Cruz, CA, USA
Vinculin	hVIN-1 / V9131	Sigma-Aldrich, St Louis, MO, USA
γ-Tubulin	GTU-88 / T6557	Sigma-Aldrich, St Louis, MO, USA

For detection of human Hdm2 we used a mix of 4B2 and SMP14 (*), for detection of human p53 we used a mix of DO-1 and 1801 (°).

Ref) Chen J *et al.* Mapping of the p53 and mdm-2 interaction domains. *Mol Cell Biol* 1993, **13:**4107-4114.

Supplementary Table 2: Primer sequences used for qRT-PCR reactions.

Gene	Forward primer	Reverse primer
p21	5'-AGCAGAGGAAGACCATGTGGA-3'	5'-AATCTGTCATGCTGGTCTGCC-3'
Noxa	5'-ACTGTTCGTGTTCAGCTC-3'	5'-GTAGCACACTCGACTTCC-3'
PUMA	5'-GACCTCAACGCACAGTA-3'	5'-CTAATTGGGCTCCATCT-3'
Bax	5'-ATGTTTTCTGACGGCAACTTC-3'	5'-ATCAGTTCCGGCACCTTG-3'
MCL1	5'-TAAGGACAAAACGGGACTGG-3'	5'-AACCAGCTCCTACTCCAGCA-3'
Wip1	5'-ATACCTGAACCTGACTGAC-3'	5'-CTCCTCCAGTGACTTGAC-3'
CAPNS1	5'-ATGGTTTTGGCATTGACACATG-3'	5'-GCTTGCCTGTGGTGTCGC-3'
RPS11	5'-AAGCAGCCGACCATCTTTCA-3'	5'-CGGGAGCTTCTCCTTGCC-3'